EurJIC European Journal of Inorganic Chemistry

ChemPubSoc Europe

MICROREVIEW

DOI:10.1002/ejic.201300285

Ligand Effects on Bonding and Ion Pairing in Cationic Gold(I) Catalysts Bearing Unsaturated Hydrocarbons

Daniele Zuccaccia,*[a] Leonardo Belpassi,*[b] Alceo Macchioni,[c] and Francesco Tarantelli[c]

Keywords: Gold / NMR spectroscopy / Ion pairs / Density functional calculations / Charge-displacement analysis / Alkenes / Alkynes

We critically review recent experimental and theoretical investigations into some key aspects of the chemistry of gold(I) complexes of the type $[L–Au–S]^+X^-$ (L = NHC carbenes and phosphanes, S = alkenes and alkynes, and X^- = weakly coordinating counterion). These systems are important intermediates formed during gold-catalyzed nucleophilic additions to an unsaturated substrate, and their specific activity is largely governed by two fundamental factors: the nature of the gold–substrate bond and the role of the ion-pair structure in solution. Both are crucially influenced by the nature and properties of the auxiliary ligand L, and on this interplay we focus our discussion. The relative anion–cation orientation, investigated by NOE NMR spectroscopy and DFT calculations, shows that the exact position of the counterion is determined by the natures of the ancillary ligand and substrate: the counterion is located near the substrate in the phosphane complexes, while for the NHC complexes the preferred position of the counterion is near the ligand. This tunable interionic structure opens the way to greater control over the properties and activity of these catalysts. The bond between Au^I and the unsaturated substrate is investigated using an original and powerful theoretical method of analysis. Our approach permits a rigorous definition and assessment of the charge-displacement (CD) components at the heart of the Dewar–Chatt–Duncanson model: substrate-to-metal (σ donation) and metal-to-substrate (π back-donation) and how these change with different ligands. The results consistently reveal that π back-donation is a large and crucially important component of the Au^I–substrate bond in all systems: π back-donation penetrates the external side of coordinated alkynes, where nucleophile attack is directed, thus partially mitigating the electron depletion caused by σ donation.

Introduction

In the last decade the use of linear gold(I) complexes in homogeneous catalysis has vastly increased.[1] Many gold-catalyzed reactions have been studied, and many have had a significant impact in the synthesis of important new molecules in various fields of chemistry. Most of these reactions, which gold(I) catalysts enable to run efficiently under extraordinarily mild reaction conditions and atom economy,[2] can be classified as nucleophilic additions to a carbon–carbon unsaturated bond. A major aim of the research has been to establish suitable and efficient reaction pathways for the construction of new organic molecules and the development of new synthetic strategies. As a result, a great amount of empirical information is now available, but the development of new catalysts still proceeds mostly by trial and error.[1c] A significant contribution towards a better understanding of ligand effects in gold catalysis has been made by Wang et al.,[3] and Fürstner et al.[4] have given an example of rational ligand design in the context of asymmetric catalysis. Several other research groups, including us, are also trying to synthesize, isolate, and characterize the chemical species that occur in the catalytic cycles. In essentially all the proposed mechanisms, the gold metal fragment acts as a Lewis acid coordinating the unsaturated carbon–carbon bond (Scheme 1, intermediate 1), which subsequently undergoes nucleophilic attack, with the formation of organogold intermediates (Scheme 1, intermediate 2). The gold–carbon bonds in these intermediates are typically cleaved by electrophiles, usually a proton, to give the desired products and regenerate the catalyst (Scheme 1).[5]

It is known that the ligand L plays a major role in tuning the reactivity and selectivity of the process,[1c,6] and certain classes of molecules, including phosphanes and N-heterocyclic carbenes (NHC) have emerged as privileged ligands for homogeneous gold(I)-mediated reactions. The electronic

[a] Dipartimento di Chimica, Fisica e Ambiente, Università di Udine,
Via Cotonificio 108, 33100 Udine, Italy
Fax: +39-0432 558803
E-mail: daniele.zuccaccia@uniud.it
Homepage: http://people.uniud.it/page/daniele.zuccaccia
[b] Istituto di Scienze e Tecnologie Molecolari del CNR (CNR-ISTM), c/o Dipartimento di Chimica, Università degli Studi di Perugia,
06123 Perugia, Italy
E-mail: belp@thch.unipg.it
[c] Dipartimento di Chimica, Università degli Studi di Perugia,
Via Elce di Sotto 8, 06123 Perugia, Italy

Supporting information for this article is available on the WWW under http://dx.doi.org/10.1002/ejic.201300285

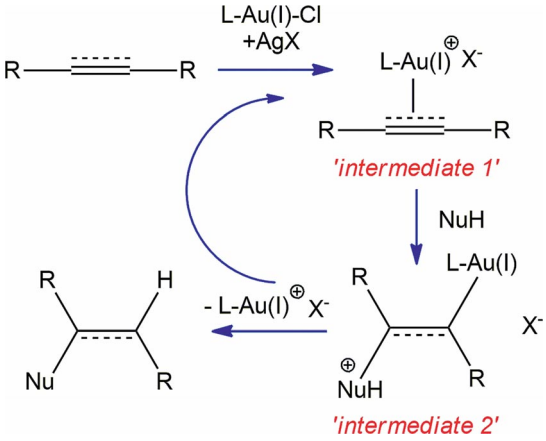

Scheme 1.

structure of the ligand, in particular its overall electron-donating ability, modulates the acidic character of the metal fragment and affects the stability of the intermediates postulated for the catalytic cycle [vinylgold compounds,[6] (carbene)gold,[7] and more or less delocalized carbocationic complexes]. A notable example of tunable ligand control in the LAu^+ fragment is provided by the class of allene dienes.[8] The picture that emerges from all these studies has been summarized by Raubenheimer and Schmidbaur.[9] Ligands that are strongly donating, such as alkyl phosphanes, are found to promote hydride migration because presumably they stabilize the carbene intermediate. On the other hand a ring contraction is found to occur when ligands that donate only weakly, such as phosphites, are used. These last probably stabilize the carbocation in the α position to the gold atom. Along the same lines, Alcarazo et al.[10] showed that the pathway of the reaction towards the products may be finely controlled by changing the electronic properties of the NHC ligands, and in particular by tuning its π-acidic property through the introduction of a cyclophane group on the imidazole ring.

The sizeable accumulation of empirical knowledge exemplified above is so far only partly accompanied by a deeper theoretical understanding of the principal factors which govern gold(I)-based catalysis. These include, first, the very nature of the gold–substrate bond, which undoubtedly makes gold so special, and how this may be tuned by the choice of auxiliary ligand. The most popular understanding of metal coordination bonds is in terms of the Dewar–Chatt–Duncanson (DCD) model of ligand-to-metal electron donation and metal-to-ligand back-donation. Great effort and much discussion have been devoted to establishing how these bond components typically balance to confer on gold its remarkable and selective activating properties, one widely held view being that gold is an especially poor back-donating agent. Experimental clues on this aspect are only indirect and often not sufficiently unambiguous, principally because both the donation and back-donation components tend to weaken the coordinated C–C bond.

A further important factor affecting the catalytic cycle is the role played by the anion (X^-). Its effect on both intermediate 1 and intermediate 2 in Scheme 1 may be crucial. Numerous examples of the influence of the anion on the cata-

Daniele Zuccaccia was born in Perugia, Italy, in 1977. He obtained his "Laurea" in Chemistry from the University of Perugia in 2001 under the supervision of Alceo Macchioni. In June 2011 he became a researcher in General and Inorganic Chemistry at the University of Udine. He has recently received the Flavio Bonati prize from the Interdivisional Group of Organometallic Chemistry of the Italian Chemical Society. His current research activities concern the synthesis, characterization, and application in homogeneous catalysis of metalloorganic compounds, with particular attention to the role of noncovalent interactions on their structure and reactivity. Since 2009, his research has focused on the synthesis and characterization of intramolecular and interionic Au^I compounds and their application in catalysis.

Leonardo Belpassi was born in Foligno, Italy, in 1977. Currently he is a researcher at CNR-ISTM, Perugia. His research interests include electronic structure calculations, relativistic effects, high-performance computing, and chemical bonding.

Alceo Macchioni is Associate Professor of Inorganic Chemistry at the University of Perugia. His research interests include the development of NMR spectroscopic methodologies for investigating the intermolecular structure of organometallics in solution, the elucidation of the relationships between structure and activity of organometallic catalysts, and the design of catalysts for the oxidation of water to molecular oxygen. In 2002 he received the Nasini award from the Inorganic Division of the Italian Chemical Society. He is author of more than 130 papers published in prestigious chemical journals (H index = 33).

Francesco Tarantelli was born in Porto San Giorgio, Italy, in 1956 and has been full professor at the University of Perugia since 2000. His research activity in theoretical and computational chemistry extends over a wide variety of subjects, including electron spectroscopy, intermolecular interactions, relativistic quantum chemistry, algorithms, and high-performance computing.

lytic activity,[11–13] the regioselectivity,[14] and even the stereoselectivity[15–17] are indeed present in the literature. In the hydroamination reaction of 1,3-dienes reported by Brouwer and He[11a] that uses [PPh_3AuCl] as precatalyst, activated by a silver salt (AgX), the efficiency was shown to be strongly dependent on the counteranion: weakly coordinating anions ($X^- = BF_4^-$, ClO_4^-, or OTf^-) give almost quantitative yields, while stronger-coordinating anions ($X^- = NO_3^-$, OTs^-) deactivate the catalyst. An impressive example, among others, highlighting the importance of ion pairing has been reported by Toste and co-workers. They showed that a high enantiomeric excess, modulated by the polarity of the solvent, can be simply achieved in the asymmetric hydroalkoxylation of allenes by the use of a chiral counterion.[16a] It may be surmised[18] that an even higher enantiomeric excess than achievable with a chiral auxiliary ligand might be obtained when a suitable anion resides near the catalytic site. But only accurate experimental indications,[19] as well as theoretical calculations, will clarify these aspects in detail.

However, although it is well recognized that ion pairing affects catalytic performance, the mechanism by which the anion actually influences the mechanism is still largely unknown. Theoretical studies proposed that the anion intervenes during the protodeauration step, but also the solvent and the nucleophilic agent itself can act as proton shuttle.[20] Different regio(enantio)selectivity seems to implicitly suggest that the chiral counterion plays a role during the nucleophilic attack rather than simply in the deauration step. For this reason, a detailed description of the anion–cation structures and interactions for all the catalytic intermediates would be highly desirable. These studies are particularly challenging because many different factors may have a significant impact on the ion-pair structure in solution. Certainly the ligands present in the first coordination sphere of the metal center play a major role, but the nature of the anion,[21] the presence of other weak interactions such as hydrogen bonding[22] and π–π stacking,[23] and the nature of the solvent[24] also contribute in unknown and varying proportions.

In our recent research, which we review in this paper, we have combined experimental and theoretical work to focus principally on the two fundamental aspects of the chemistry of gold(I)-based catalysts outlined above, namely the properties of the gold–substrate bond and the extent and role of ion pairing. Our efforts have been directed at explaining how these features are influenced, and may be tuned, by a proper choice of the ligand L. One of the main results of this work has been the development of a simple theoretical approach, charge-displacement (CD) analysis, capable of fully characterizing the metal–substrate bond.[25] The method provides a clear picture of the electron-density redistribution accompanying gold–carbon bond formation and, thereby, a quantitative measure of the varying ability of the metal–L fragments to act as electron acceptors toward the unsaturated CC bond of a substrate. Even more interestingly, the method has been extended to provide an unambiguous measure of the DCD donation and back-donation components of the coordination bond, with novel, extremely illuminating and at times surprising results.[26] This analysis also casts some light on the correlation between the ion-pair structure and the acidic strength of the $L–Au^+$ fragment, as well as paving the way for a better explanation of the connection between the ligand effect on the gold–substrate bond and some experimental observables.

Our experimental work makes use of advanced NMR spectroscopic techniques such as NOE[27–29] and pulsed field gradient spin-echo (PGSE) NMR spectroscopy,[30] which we have developed[31] and found particularly suitable for gaining detailed information on the relative anion–cation orientation in solution and on the degree of aggregation of the organometallic compounds. Combined with extensive computational studies of the potential energy surfaces and Coulomb potential of the ions, these approaches give detailed information on the structure and on the strength of the ion pairs and may also help in characterizing the most important interactions at the origin of a given ion-pair structure.[32–34] Both phosphane and carbenes have been investigated as effective ligands, showing that the anion position is strongly affected by the ligand and may be finely modulated, with varying intensity, by substituent groups.

Ion Pairing

Ion pairing critically affects the structure and reactivity of ionic transition metal complexes, particularly in low-polar solvents.[31] Over the last few years we have been developing investigative methodologies that take advantage of the complementary information from diffusion and NOE NMR spectroscopy to disclose the structure of ion pairs in solution.[27] The method has been successfully applied to investigate several classes of ionic transition metal complexes with different metals, ligands, and geometries.[30] Remarkable results have been obtained for organometallic catalysts for alkene polymerization[35] and alkene/CO copolymerization[36] in terms of explanation and, in some cases, correlation between the ion-pair structure and the reactivity.

More recently we started to apply the same method to the study of gold ion pairs. In particular, we focused on $[L–Au–S]^+X^-$ ion pairs (L is the ancillary ligand, S is the unsaturated substrate, and X^- is the counterion) and attempted to combine advanced NOE NMR spectroscopic measurements in solution and theoretical calculations made by DFT. NOE NMR spectroscopy, based on the detection of dipolar interactions, is ideal for measuring the spatial proximity of two (or more) NMR-active (I and S) nuclei, regardless of whether I and S are in the same molecular fragment (intramolecular NOE) or belong to two different moieties (intermolecular NOE). This means that the relative anion–cation orientation(s) within an ion pair can be disclosed if (i) NMR-active nuclei, possibly with high receptivity (i.e. hydrogen or fluorine), are present in both ionic

moieties, (ii) they are not homogeneously distributed (non-equivalent) around the ionic moieties, and (iii) their maximum internuclear distance is no more than approximately 5 Å. The last is not a severe limitation, since ion-pairing effects are important almost exclusively when mainly contact ion pairs are present in solution. The NOE interionic contacts can be classified as strong, medium, or weak, according to the intensity of the crosspeaks. Quantification of I/S interionic NOE intensities with respect to that of an A/B intramolecular peak, where A and B are two nuclei, with interacting dipoles, for which the internuclear distance is known, allows the average internuclear distance (r_{IS}) to be determined according to Equation (1).

$$r_{IS} = r_{AB}\left\{\frac{NOE_{AB}}{NOE_{IS}}\right\}^{\frac{1}{6}} \quad (1)$$

NOEs in Equation (1) must be scaled, considering that they are proportional to $[n_I n_S/(n_I + n_S)]$, where n_I and n_S are the number of equivalent I and S nuclei that undergo a dipolar interaction, respectively.[37]

In deriving Equation (1) it is assumed that the two nuclear couples, I/S and A/B, have the same correlation time (τ_c). This is not necessarily true since, while A and B belong to the same molecular fragment, I and S are in two non-covalently bonded moieties (anion and cation in an ion pair). An estimate of τ_c is necessary in order to obtain accurate interionic distances. The procedure of quantifying interionic NOEs leads to remarkably accurate interionic distance measurements and provides information not obtainable with any other experimental technique.[35a] For example, quantification of interionic NOEs in [PtMe(η^2-4-$CF_3C_6H_4CHCH_2$)(α-diimine)]BF_4 complexes allowed direct observation of an equilibrium between two anion–cation orientations and evaluation of its ΔG, which was always less than 1 kcal/mol.[38]

The potential of NOE NMR spectroscopic studies can be further exploited if they are paralleled with theoretical calculations.[39] In particular, in the last few years we have shown that analysis of the charge distribution on the cation is often sufficient on its own to obtain a reliable indication of the most favored sites for anion–cation interactions. Our approach has therefore been to map the Coulomb potential generated by the isolated complex $(L–Au–S)^+$ in a region accessible to the anion and match this with the results of the experimental measurements. A reasonable choice is to map the Coulomb potential on the electronic isodensity surface that is approximately tangent to the equivalent density surface of the isolated anion placed at the optimized geometry of the ion pair. This can be considered to yield a map of the potential on a boundary roughly corresponding to the steric dimension of the cation. When more quantitative information is required or some specific interactions between the anion and cation exist, one has to resort to the analysis of the actual cation–anion potential energy surface. Typically several, often computationally expensive, geometry optimizations within an appropriate solvation model are necessary (see Supporting Information).

All the $[L–Au–S]^+X^-$ ion pairs synthesized and studied in our laboratory are reported in Scheme 2. Their interionic structures in solution have been determined by means of NOE NMR spectroscopic experiments carried out in CD_2Cl_2. In all cases BF_4^- was used as the counterion. Analogous complexes have been synthesized by others[40] using phosphanes,[41] N-heterocyclic carbenes (NHCs),[42] and cyclic (alkyl)(amino)carbenes (CAACs)[43] as ancillary ligands and alkenes,[44] alkynes,[45] arenes,[46] dienes,[47] and allenes[48] as substrates. Complexes **1**BF_4 and **2**BF_4 were generated in situ within an NMR spectroscopy tube at low temperature and immediately analyzed, in order to avoid their rapid decomposition to metallic gold and $(L–Au–L)^+$.

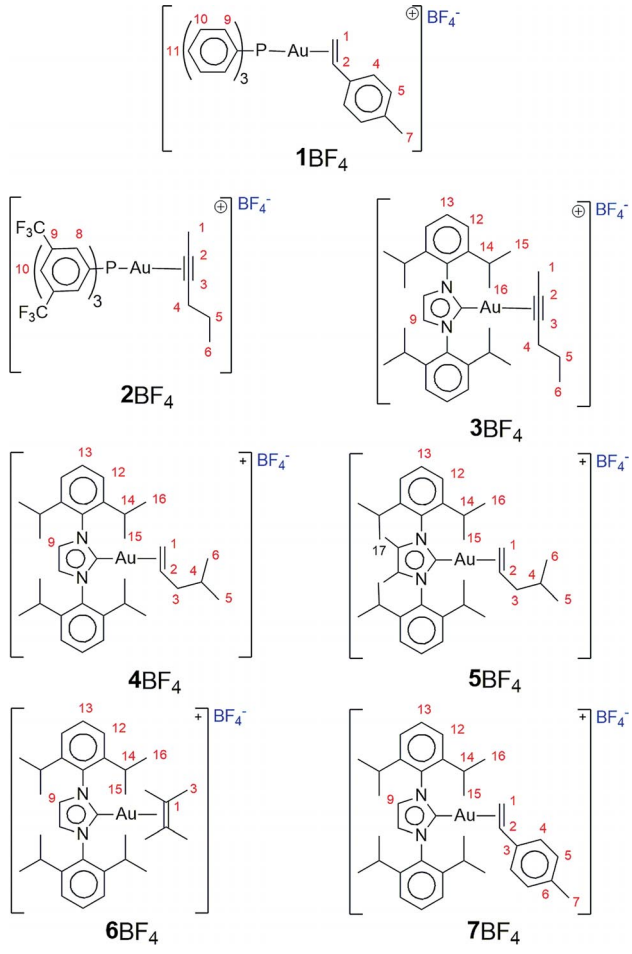

Scheme 2.

Although PPh_3 is widely used as ancillary ligand in homogeneous catalysis with gold, **1**BF_4 and **2**BF_4 are the only PPh_3 ion pairs cleanly generated and characterized. By contrast, complexes **3**BF_4–**7**BF_4, with alternative ligands, were synthesized, isolated, and characterized. $[NHC–Au–S]^+X^-$ species are rather more stable than their phosphane analogs. This allowed a systematic investigation of the interionic structure of $[NHC–Au–S]^+BF_4^-$ ion pairs to be carried out, with the aim of understanding how steric and electronic properties of both the NHC ligand and the substrate modulate the ion pair structure.

As a first approximation the most important relative ion-pair orientations possible for a linear cationic fragment are sketched in Figure 1: in the relative anion–cation orientations A and C the anion is located near the ligand L or the substrate S, respectively, and in orientation B the anion is near the gold atom. The NOE data have been interpreted with respect to these three representative orientations.

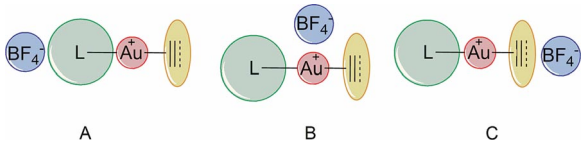

Figure 1. Three orientations, A, B, and C, of the counterion in (L–Au–S)BF_4 complexes.

The $^{19}F,^{1}H$ HOESY NMR spectra of **1**BF_4 and **2**BF_4 are reported in Figure 2 and Figure 3, respectively. In the case of complex **1**BF_4, strong contacts are observed between the F nuclei of the counterion and resonances 1*cis*, 1*tr*, and 2 of 4-methylstyrene and resonance 9 of the phosphane ligand (Figure 2). Contacts of medium intensity are also observed between the counterion and resonances 4 and 10. The analysis of these interionic NOE signals, normalized for the number of the magnetically equivalent nuclei (Table 1), shows that in complex **1**BF_4 the counterion is located mainly on the side of 4-methylstyrene and, particularly, close to the alkene region and opposed to the 4-MePh group. The picture is nicely confirmed by inspection of the map of the Coulomb potential generated by the isolated cation (Figure 4, left). The most attractive regions on the surface (blue) are located at the hydrogen atoms of the alkene. The region around the gold atom is not particularly attractive. The formal positive charge of gold(I) is clearly spread out and shared by the ligand and substrate. This is confirmed by an atomic charge analysis, which indicates that the gold atom indeed presents a positive charge smaller than 0.2, regardless of the theoretical method used.[32,33]

In the complex **2**BF_4 the ion-pair structure derived by $^{19}F,^{1}H$ HOESY NMR spectrum is even more specific. A very strong contact is present between the fluorine atoms of the counterion and protons 8 of the phosphane ligand (Figure 3). Medium-strength contacts are observed between BF_4^- and protons 1, 4, and 10. The relative intensity analysis of the NOE data (Table 1) shows that the NOE intensity between the anion and protons 8 is about ten times stronger than the others. **2**BF_4 is particularly suitable for attempting a more quantitative analysis of the experimental NOEs and for estimating the average H···F interionic distance. This is made possible by the fact that the system presents fixed intramolecular distances CF_3···proton 8 or CF_3···proton 10 in the cation, which can be used as reference, and specific contacts in the spectrum. The average H···F_4B distances for protons 1, 4, and 8 thus estimated from the NOE measurements are 4.9, 5.3, and 3.7 Å, respectively. These distances are consistent with BF_4^- being preferentially located in the space around the gold atom between the phosphane and alkyne ligands, slightly closer to the phosphane. This quantitative result was confirmed by theoretical calculations. In this case, we investigated the potential energy surface by carrying out several geometry optimizations in solution at the DFT level starting from different relative cation–anion configurations. The most stable configuration (Figure 5a) is obtained for the anion approaching the cation $\mathbf{2}^+$ in the space around gold between the phosphane and the alkyne ligands, pointing towards proton 8 of the phenyl substituent. There are also other stable configurations, close in energy to the previous one, for BF_4^- always approaching the 8 protons (Figure 5b, c, d). Configuration e (Figure 5e) with the anion that stays close to the triple bond on the opposite

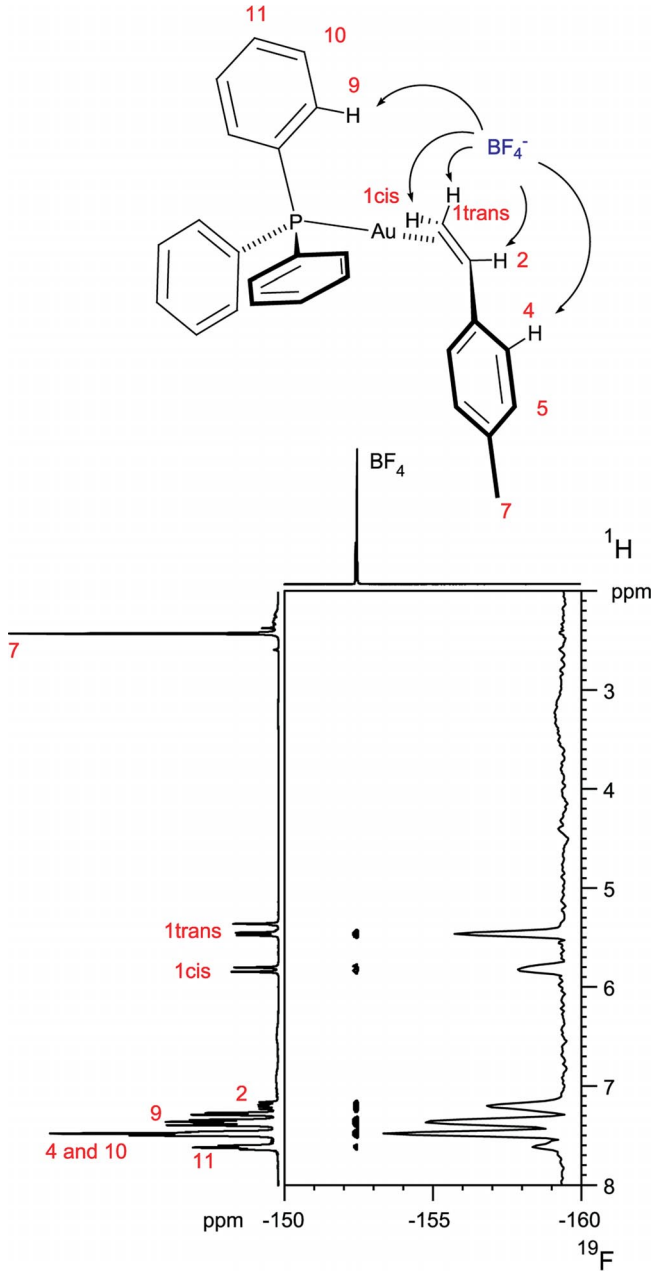

Figure 2. $^{19}F,^{1}H$ HOESY NMR spectrum (376.65 MHz, 253 K, CD_2Cl_2) of complex **1**BF_4. The column projection is reported on the right. Reproduced with permission from ref.[32] Copyright (2009) American Chemical Society.

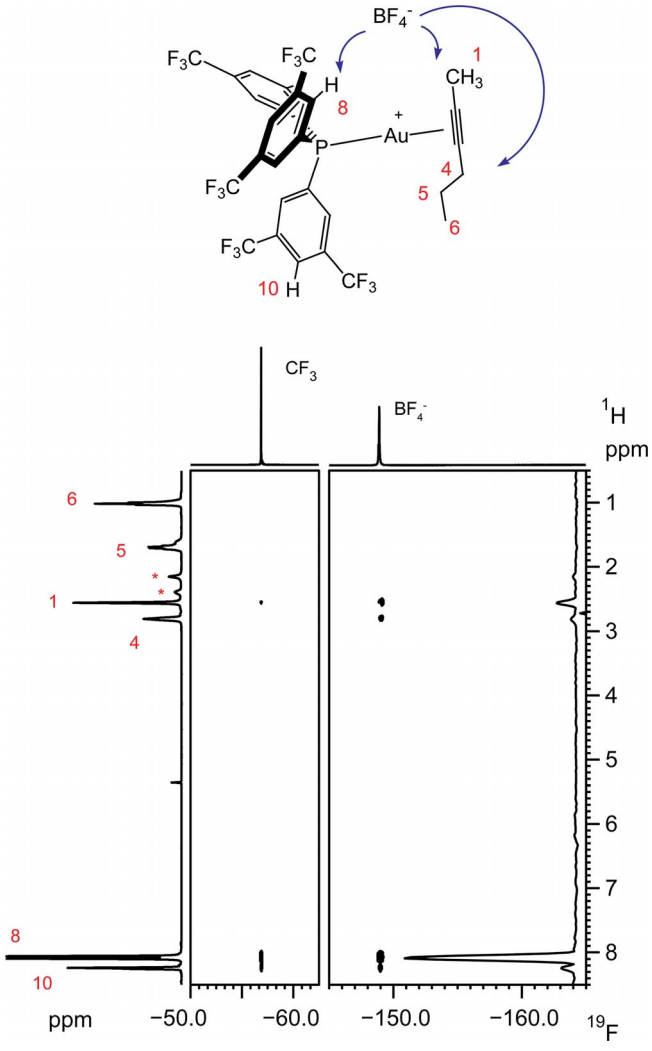

Figure 3. Two sections of the $^{19}F,^{1}H$ HOESY NMR spectrum (376.65 MHz, 204 K, CD_2Cl_2, 200 mM) of complex **2**BF_4. The F1 projection relative to the BF_4^- resonances is reported on the right. * denotes the resonances of free 2-hexyne. Adapted with permission from ref.[33] Copyright (2010) American Chemical Society.

Table 1. Relative NOE intensities determined by arbitrarily fixing the intensity of the NOE signal(s) between the anion resonances and the imidazolium protons 9 at 1 for **1**BF_4, **3**BF_4, **4**BF_4, **6**BF_4, and **7**BF_4, between the anion resonances and the imidazolium protons 17 for **6**BF_4, and between protons 8 and anion resonances for **2**BF_4.

Proton	**1**BF_4[32]	**2**BF_4[33]	**3**BF_4[33]	**4**BF_4[34]	**5**BF_4[34]	**6**BF_4[34]	**7**BF_4[32]
1*tr*	1.92	0.14	0.17	0.21	0.54	–	0.15
1*cis*	1.11					–	0.27
2	1.80			0.16	0.36	0.20	0.27
3				0.18	0.48	–	–
4	0.90	0.06	0.13	[a]	[a]	–	0.27
5(6)			0.05	0.06	0.15	–	0.20
7				–	–	–	0.13
8		1.00		–	–	–	–
9	1.00	–	1.00	1.00	–	1.00	1.00
10	0.90	0.12[b]	–	–	–	–	–
11	0.28		–	–	–	–	–
12	–	–	0.21	0.26	0.57	0.22	0.22
13	–	–	0.16	0.08	0.27	0.15	0.08
14	–	–	0.18	0.30	0.79	0.20	0.14
15	–	–	0.55[c]	0.80[c]	1.4[c]	0.55[c]	0.49
16	–	–					0.37
17	–	–		–	1.00	–	–

[a] Partially superimposed with protons 15 and 16. [b] Overestimated because of the partial overlap with proton 8. [c] Value refers to both protons 15 and 16.

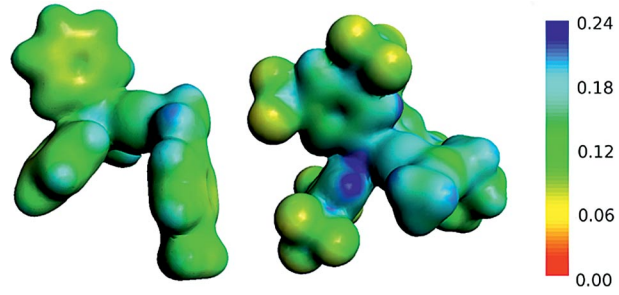

Figure 4. Different views of the Coulomb potential of **1**$^+$ (right) and **2**$^+$ (left). Adapted with permission from refs.[32,33] Copyright (2009, 2010) American Chemical Society.

side of the phosphane and far away from the protons 8 is higher in energy (by more than 0.8 kcal/mol). The configuration in which the anion is located on the PAr^F_3 ligand side (Figure 5f) is even higher in energy, by about 1.7 kcal/mol. The calculations of interionic distances were performed for the five most stable configurations weighted by their relative energy,[49] and yielded 4.5, 5.6, and 4.1 Å for 1, 4, and 8 respectively, in good agreement with the estimates derived from the NOE experiments. Calculations also show that the electron-withdrawing CF_3 groups induce a strong positive Coulomb potential at the site of the *ortho* protons 8 (blue in Figure 4), changing the overall electrostatic behavior and resulting in a specific B-type ion-pair structure (Figure 1).

Generally the anion locates preferentially on the side of the NHC ancillary ligand or, to a smaller extent, close to the unsaturated substrate in [NHC–Au–S]BF_4 ion pairs. The relative anion–cation orientation of **3**BF_4–**7**BF_4 in solution was investigated by combining information from $^{19}F,^{1}H$ HOESY NMR spectroscopic measurements and analysis of the Coulomb potential of the cation. NOE interactions for complex **3**BF_4 are depicted in Figure 6. A very similar pattern of signals was obtained for complexes **4**BF_4–**7**BF_4. The picture that emerges is clear: two possible relative anion–cation orientations are present, one having BF_4^- located at the NHC side[50] (orientation A, Figure 1) and the other with it at the substrate side (orientation C, Figure 1). Orientation B in Figure 1 is not probable because the aryl moieties with hindered *ortho* substituents[36,38,51] introduce steric encumbrance above and below the metal center. Since protons 9 of the NHC ligand are slightly acidic they carry some additional positive charge and may act as attractors for the anion, thus favoring orientation A of Figure 5. At the same time, the excellent electron-donating properties of the NHC decrease the Lewis acidity of the NHC–Au^+ moiety. As a consequence, the substrate electron

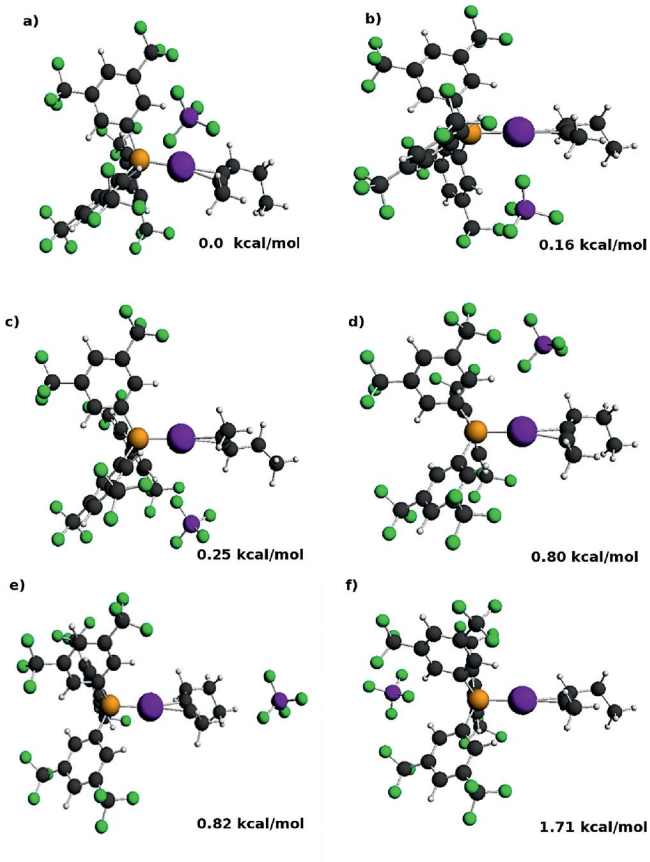

Figure 5. Stable ion-pair configurations of **2**BF_4, with their computed energy relative to the most stable structure. Reproduced with permission from ref.[33] Copyright (2010) American Chemical Society.

density is not greatly depleted and it does not seem so "appealing" to the counterion. This effect too favors orientation A.

The relative abundance of A and C orientations was determined by an analysis of the interionic NOE intensities (Table 1). Assuming that the minimum distance between the anion and the cation is the same in both orientations,[38] we estimated the abundances by the normalized NHC/anion and substrate/anion NOE intensities. Protons 9 (and 17) were chosen as the probes of the A orientation for complexes **3**, **4**, **6**, **7** (and **5**). The protons showing the largest NOEs were selected as probes for the orientation C. For complex **3**BF_4 the intensity ratio of NOE signals is 1:0.17 (Table 1), leading to estimated abundances of the A and C orientations equal to 86% (1.00/1.17 × 100) and 14% (0.21/1.21 × 100), respectively. DFT calculation showed that, despite the fact that the configuration A – with the anion near the imidazole ring – is still the most stable, configuration C is only 0.5 kcal/mol higher in energy and so may easily accessible.

In the case of complex **4**BF_4, the intensity ratio of the BF_4^-···proton 9 and BF_4^-···proton 1*tr* NOE signals leads to a very similar relative abundance of the A and C orientations, 83% (1/1.21 × 100) and 17%, respectively. Consistent with this, protons 9 have the most positive Coulomb potential (Figure 7) while protons 1*cis*, 1*tr*, and 2 are the most electropositive protons of the alkene fragment.

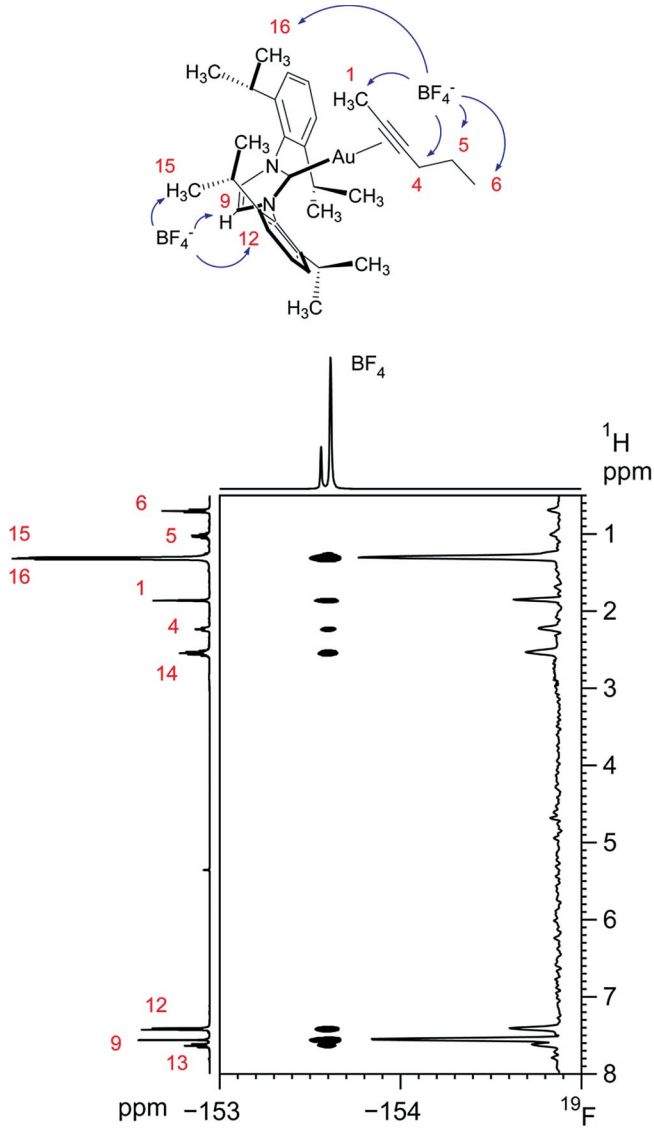

Figure 6. ^{19}F,^1H HOESY NMR spectrum (376.65 MHz, 298 K, CD_2Cl_2, 61 mM) of complex **3**BF_4 showing the interionic NOE signals of the counterion with protons 9 (strong), 12 (medium), 14 (medium), 15 (16) (medium/strong), 1 (weak), 4 (weak), and 13 (weak). The F1 projection relative to the BF_4^- resonances is reported on the right. Reproduced with permission from ref.[33] Copyright (2010) American Chemical Society.

The ion-pair structure displays a similar pattern for both alkyne and alkene substrates, showing that the ion-pair structure, at least in this case, is unaffected by the degree of unsaturation of the C–C bond. The comparison between the interionic structures of complexes **4**BF_4, **6**BF_4, and **7**BF_4 allows us to explore the possible effects of substituents on the alkene in the ion-pair structure. In the reality, the presence of methyl groups in **6**BF_4 or of an aliphatic substituent bound to the double bond in **7**BF_4 does not alter the picture significantly. The Coulomb potential (Figure 7) shows that the methyl groups bound to the double bond offer an extended positively charged area for anchor-

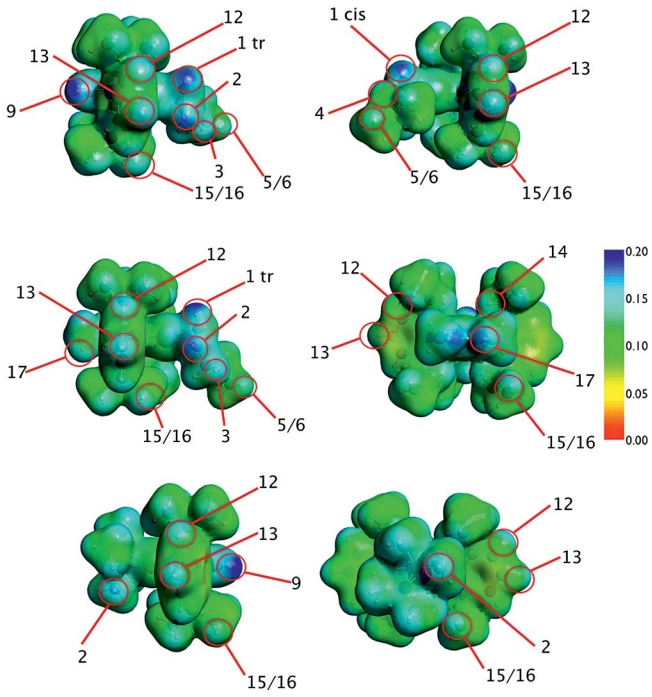

Figure 7. Different views of the Coulomb potential of $\mathbf{4}^+$ (top), $\mathbf{5}^+$ (middle), and $\mathbf{6}^+$ (bottom). Reprinted from ref.[34] with permission from Elsevier.

ing the anion (orientation C). A closer analysis of the NOE intensities for the alkene protons (see NOE values for proton 1*cis*, 1*tr*, and 2), however, reveals a tiny difference in the anion location in orientation C in $\mathbf{4}BF_4$ and $\mathbf{7}BF_4$ ion pairs, even if the relative abundances are fairly similar (orientations A/C about 83%:17% and 79%:21%, respectively). In the former, the anion appears to sit slightly closer to the alkene CH_2 moiety, while in the latter it is shifted towards proton 2, approaching the aryl substituent of the alkene. This difference could be due to the enhanced acidity of proton 2 caused by the electron-withdrawing nature of the aryl substituent and to the presence of more slightly positive neighboring protons (4 and 5) in $\mathbf{7}BF_4$.

Finally, ion pair $\mathbf{5}BF_4$ was synthesized and studied in order to check whether the ion-pair structure in solution could be deliberately tuned to affect the reactivity. The acidic protons 9 were replaced by methyl groups in $\mathbf{5}BF_4$ in order to force the anion to move onto the substrate side (orientation C in Figure 1). In reality, orientation A is indeed favored in $\mathbf{5}BF_4$. Again, the most intense NOE signal was observed between the anion and protons 17, but the intensity of the signal from proton 1*tr* is up to about half of that from protons 17 (Table 1), leading to a significant increase in the abundance of orientation C (35%). This almost doubles the result for $\mathbf{4}BF_4$ (about 17%). As one might expect, the Coulomb potential maps for cation $\mathbf{5}^+$ (Figure 7, middle) clearly show that protons 17 are less positively charged than protons 9 in $\mathbf{4}^+$; however, the nine protons present (protons 17 and 16) still make a rather good anchor point at which the anion can be easily trapped (Figure 7).

In summary, it can be concluded that the anion–cation orientation is mainly determined by the nature of the ancillary ligand L. When L is phosphane the anion preferentially locates close to the substrate (orientation C) and/or above and below the metal (orientation B). In contrast, when L is NHC the anion tends to stay near the ligand (orientation A).

Electronic and steric features of both L and S finely modulate the exact position of the anion. For example, the presence of CF_3 electron-withdrawing groups in $\mathbf{2}BF_4$ causes a shift of the counterion, which tends to locate close to the gold atom (orientation B) because of the presence of the rather acidic protons 8, whereas complex $\mathbf{1}BF_4$ with the PPh_3 ligand prefers to adopt orientation C. In the case of NHC-bearing ion pairs, the substitution of the rather acidic protons 9 of the NHC with methyl groups causes a decrease of the abundance of orientation A from 83% to 65%.

Bond Characterization: Charge-Displacement Analysis

A growing body of theoretical data exists on gold chemistry,[52] but an understanding of the nature of the chemical bond between Au and the substrate in the catalytic intermediates is still limited and lacks predictive capacity.[53] In recent years, we have used a novel approach that has proved capable of providing new insights and settling some long-standing questions. Our method combines relativistic quantum chemical calculations with a detailed analysis of the change in electron density due to the metal–carbon bond formation. This provides an objective estimate of the charge transfer between gold and its ligands that is independent of any charge-decomposition model. As will be reviewed in the second part of this section, a simple generalization of this analysis to different symmetry components is also often possible, and this gives a picture of the gold–carbon bond from which the ligand-to-metal donation and metal-to-ligand back-donation contributions emerge naturally. This provides, for the first time, an actual rigorous definition and measure of the bonding components of the DCD model.

The key idea of our approach is concisely expressed by the CD function along a given direction z.

$$\Delta q(z) = \int_{-\infty}^{+\infty}\int_{-\infty}^{+\infty}\int_{-\infty}^{z} \Delta\rho(x,y,z')\,dx\,dy\,dz' \qquad (2)$$

$\Delta\rho\,(x,y,z')$ is the difference between the electron density of a complex and that of its noninteracting fragments placed in the same position they occupy in the complex. The defined fragments in this case are the L–Au^+ (or L–Au in the case of an anionic ligand) moiety and the alkyne substrate. The function $\Delta q(z)$ was successfully introduced to study the chemical bond between gold and the noble gases[25] and was also used to investigate charge transfer in weakly bound water adducts.[54]

The physical meaning of the function $\Delta q(z)$ is clear: it defines, at each point z along a chosen axis, the amount of

electronic charge that, upon formation of the bond, has moved across the plane perpendicular to the axis through the point z. A positive (negative) value corresponds to electrons flowing in the direction of decreasing (increasing) z.

In Figure 8 we begin by reporting the 3D contour plots of the electron-density difference, $\Delta\rho(x,y,z)$, between complexes **2**$^+$, **3**$^+$, and their respective noninteracting fragments. The neutral complex [AuCl-(2-hexyne)] is also presented as a reference. The isolated fragments making up the unperturbed density are the 2-hexyne and, respectively, $(PAr^F{}_3)Au^+$ in **2**$^+$, $NHCAu^+$ in **3**$^+$, and AuCl in [(AuCl)-(2-hexyne)] at the geometry they have in the respective complexes. In all cases the electron density has been evaluated at the DFT level including relativistic corrections (see ref.[33] for details). Figure 8 shows clearly that, upon coordination, a significant charge rearrangement takes place at both gold and alkyne sites. The triple bond of the substrate is strongly polarized towards the gold site, with a charge accumulation (blue) in the bonding region, and an evident decrease of electron density (red) at the opposite side, the outer part of the triple bond in the alkyne, which is thus made suitable for a nucleophilic attack. It is remarkable that a certain amount of charge depletion at the alkyne site is present even for the neutral complex, which is indeed used effectively in catalysis for activating unsaturated CC bonds. The CD curves [Δq; see Equation (1)] give us a quantitative picture (Figure 9) of the actual charge redistribution due to the formation of the coordination bond and of the electron-withdrawing ability (Lewis acidity) of the metal fragment L–Au^I towards the unsaturated substrate. The three complexes do indeed differ significantly and quantitatively because of the presence of different ligands.

The curve for complex **2**$^+$ (with a phosphane ligand) is consistently more positive than those of complex **3**$^+$ (with a NHC ligand) and the neutral complex [AuCl-(2-hexyne)]. Note further how this pattern extends to the whole molecular region. The curves illustrate well the fact that the scarcer the electron-donating ability of the ligand is, the stronger the Lewis acidity of the metal fragment is. In order to quantify this, in particular for the purpose of discussing charge transfer (CT) between the alkyne and the L–Au$^+$ moiety, it is useful to fix some plausible boundary separating the fragments in the complexes. A reasonable choice is represented by the vertical yellow band in Figure 9. This marks a zone, of width equal to about one tenth of the Au–alkyne distance, around the z point of tangency of the equal-valued isodensity surfaces of the isolated fragments of each complex. At this isodensity boundary, we see that complex **2**$^+$ is characterized by a net donation of about 0.25 electrons from 2-hexyne to the $(PAr^F{}_3)Au^+$ fragment (within the band, CT actually varies slightly between 0.23 and 0.26 electrons). Complex **3**$^+$ displays a smaller net donation of about 0.15 electrons (the interval is 0.14–0.17 e), while the neutral complex [AuCl-(2-hexyne)] is characterized by roughly half this CT value (0.06–0.09 e). Remarkably, the much more pronounced electron loss of the alkyne in **2**$^+$ is not only observed at the boundary but, perhaps even more interestingly, persists at the triple bond site.

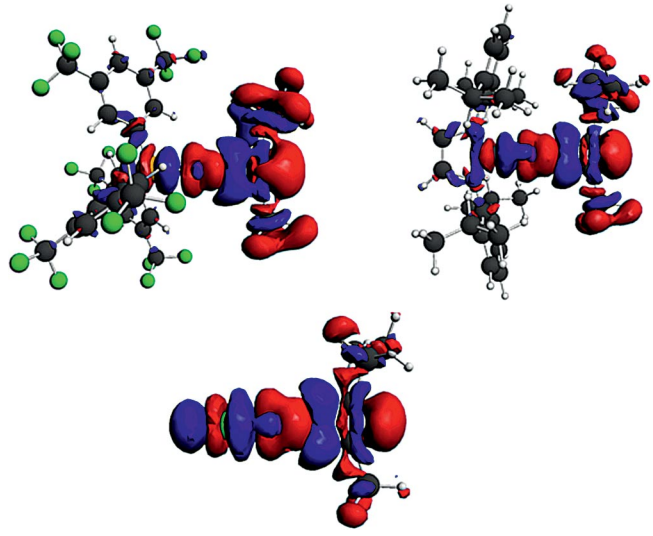

Figure 8. Three-dimensional plot of electron-density difference for **2**$^+$ (left), **3**$^+$ (right), and [AuCl-(2-hexyne)] (bottom).[33] Red isosurfaces identify where the electron charge is depleted with respect to the fragments $(PAr^F{}_3)Au^+$ and 2-hexyne for **2**$^+$, $NHCAu^+$ and 2-hexyne for **3**$^+$, and AuCl and 2-hexyne for [AuCl-(2-hexyne)]. The zones of density accumulation are marked with blue isosurfaces. Density value at the isosurface: ±0.0008 a.u. Adapted with permission from ref.[33] Copyright (2010) American Chemical Society.

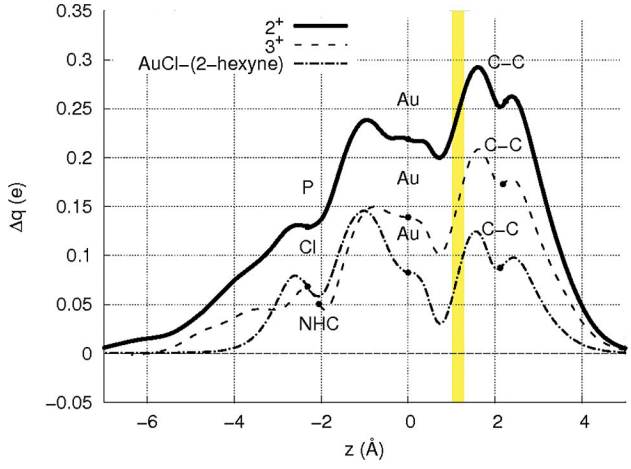

Figure 9. CD curves for the three complexes. Adapted with permission from ref.[33] Copyright (2010) American Chemical Society.

As we said above, one may expect that an alkyne coordinated at the $PAr^F{}_3Au$ moiety is more susceptible to nucleophilic attack, accelerating the reactions in which alkyne activation is the rate-determining step. This is indeed the case, for instance, in the hydration of alkynes to ketones,[55,56] the kinetics for which appears to be indeed dominated by alkyne activation.[20c] The deactivation of the catalyst is also crucial for the overall catalytic performance, and **3**BF_4, with a NHC ligand, appears to be particularly kinetically stable, despite a smaller net acidity, as confirmed by the mild experimental conditions of preparation. These findings support the view that catalysts with phosphane ancillary ligands (poorer electron donors) are more effective in activat-

ing alkyne substrates (higher turnover frequency, TOF), while NHC–gold systems may act as effective catalysts because, despite their poorer net acidity, they are more robust (higher turnover number, TON).

The net acidity of the metal fragment and its tuning by a suitable choice of ligand are thus important factors in the activation of multiple bonds. One should not overlook the fact that the net acidity may result from the contribution of two fluxes of electron density in opposite directions. These are the bonding components of the well-known DCD model. As mentioned in the Introduction, the interpretation of the electronic structure of gold complexes in terms of the extent and relative importance of substrate-to-metal [S→AuL] donation and metal-to-substrate [LAu→S] back-donation is the subject of an apparently never-ending controversy. Experimental clues about the bonding are only indirect even in the simplest cases. The alkyne→M donation and M→alkyne back-donation components both tend to weaken the C–C bond, so that simple spectroscopic parameters such as the C–C bond length or stretching frequency obtained by Raman or IR spectroscopy, which are commonly used for the characterization of these species, are not particularly helpful for obtaining insights into the nature of the interaction. Many authors have suggested that the peculiar catalytic properties of gold(I) may originate from a negligible propensity for back-donation since, quite simply, this would increase the electrophilicity of the coordinated substrate.[57] These suggestions are, however, mostly unsupported, and were often just based on the observation that gold(I) carbonyls are "nonclassical", having a blueshifted CO stretching frequency. But this blueshift is mainly caused by the polarization of the C–O bond due to the Au positive charge, which strengthens the covalent interactions in the CO moiety.[58]

Available X-ray crystallographic structures for complexes containing an alkyne coordinated to gold(I) (see ref.[9] and references cited therein) show, quite surprisingly, that the distortion of alkynes from linearity is even larger in neutral than in cationic complexes having phosphanes or NHC ligands. The neutral AuCl and $[N\{(C_3F_7)C(Dipp)N\}_2Au]$ complexes reported by Dias et al.[45a,45b] induce a bend in coordinated 3-hexyne resulting in a C≡C–C angle of 165° and 155°, respectively. The corresponding angles in NHC– and phosphane–gold complexes are typically smaller, with deviations of the alkyne from linearity of 9–14°.[41d,42d] DFT calculations support these structural observations and in addition show that the interaction energies between the metal fragment and the alkyne vary surprisingly little, being almost independent of the various ligands. For instance, in the case of complexes **1**, **2**, and AuCl interacting with 2-hexyne, the structures and interaction energies we computed show a similar pattern to that measured by experiments: deviations from linearity are 12.7°, 13.8°, and 15°, while the interaction energies are 38.1, 37.4 and 36 kcal/mol, respectively. This experimental and theoretical evidence cannot be explained solely on the basis of the net acidic properties of the metal fragment. In fact, it suggests instead a specific role of metal-to-substrate back-donation.

We started to investigate precisely these aspects and extended the CD analysis approach to directly identify and measure the spatial distribution of the alkyne→M donation and M→alkyne back-donation components in these systems. We applied this analysis to the series of coinage-metal bilinear complexes, of formula L–M^I–ethyne, with L = Cl^-, NHC (2,3-dihydroimidazol-2-ylidene), and M = Cu^I, Ag^I, and Au^I (Scheme 3).[26] We also present here for comparison some new results concerning the complex with a simple phosphane, PH_3–Au^I–ethyne. Our approach is based on the application of CD analysis on different molecular symmetry components. The use of symmetry permits the separation of the total $\Delta\rho$ function into components according to Equations (3) and (4).

$$\Delta\rho = \sum_p \Delta\rho_p \tag{3}$$

$$\Delta\rho_p = \sum_{i\in p} \left|\phi_i^{(AB)}\right|^2 - \sum_{i\in p} \left|\phi_i^{(A)}\right|^2 - \sum_{i\in p} \left|\phi_i^{(B)}\right|^2 \tag{4}$$

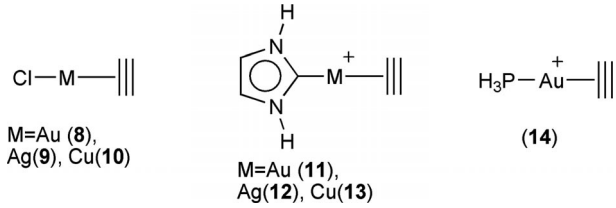

Scheme 3.

Here p labels the symmetry-irreducible representations of a complex AB and its fragments A and B (the symmetry is the same in the cases studied here), while ϕ_i are the Kohn–Sham orbitals.

For simplicity we considered the complexes **8**–**14** in C_s symmetry with the symmetry plane chosen as the plane perpendicular to the C≡C bond of ethyne and containing the gold atom. The z axis is that passing through gold and the C≡C midpoint. The separation of the Δq function into the two irreducible representations A′ and A″ thus provides a rigorous definition of the components of the DCD bond model. Table 2 summarizes the results extracted by the CD analysis for several systems of formula L–M^I–ethyne. In Figure 10 the CD curves for the complexes [Cl–Au–ethyne], $[NHC–Au–ethyne]^+$, and $[PH_3–Au–ethyne]^+$ are reported.

The CD curves obtained for A′ symmetry are positive and large everywhere, describing unambiguously a net flux of electronic charge from the alkyne towards the metal fragment (from right to left). This gives a detailed picture of the spatial distribution of the alkyne-to-metal donation (blue lines in Figure 10). This symmetry correlates with the filled in-plane and out-of-plane occupied π orbitals of the alkyne fragment. By contrast, the CD curves for A″ symmetry are negative in the whole Au–ethyne bond region,

Table 2. Computed S→M donation and M→S back-donation values (in electrons) extracted from the CD curves of the [L–M–ethyne] complexes at the boundary between the fragments defined in the text. Reproduced with permission from ref.[26] Copyright Wiley-VCH Verlag GmbH & Co. KGaA.

Complex	S→M	M→S	Total
8	0.26	0.23	0.03
9	0.18	0.13	0.05
10	0.20	0.22	–0.02
11	0.25	0.13	0.12
12	0.18	0.06	0.12
13	0.20	0.13	0.07
14	0.27	0.10	0.17

describing a reverse flux of electronic charge from the metal fragment to the alkyne site. This symmetry consistently correlates with empty in-plane and out-of-plane π* orbitals of the free alkyne (red lines in Figure 10).

The picture emerging from this analysis could not be clearer in showing that π back-donation constitutes a large component of the gold(I)–carbon interaction. It does indeed have a pronounced negative peak in the region between the gold atom and the alkyne. The result is that the total CD, the net acidity, arises from the delicate balance of large opposite donation and back-donation components. Despite a similar qualitative picture, the three complexes (**8**, **11**, and **14**) present some remarkable differences due to the different electronic properties of the ligands. If we focus on the bond region between the two fragments, where we draw the isodensity boundary between the LAu^I and ethyne fragments (yellow vertical band), we can see that the complexes exhibit nearly identical alkyne-to-metal donation. At the middle of the yellow band this component is 0.26, 0.25, and 0.27 e for **8**, **11**, and **14**, respectively, in spite of the remarkable difference in the net charge transfer (0.03, 0.12, 0.17 e). π back-donation is much larger for the neutral complex **8** (about 0.23 e), so that it almost cancels out the donation, almost half as much (0.12 e) in complex **11**, and even lower (0.10 e) in the complex with phosphane **14**. The ratio of total donation to back-donation changes from 1.1 in the neutral complex **8**, to 1.9 in **11** and 2.7 in **14**.

The view that attributes the remarkable catalytic properties of Au^I in activating multiple C–C bonds to a small π back-donation component of the bond must clearly be abandoned. Furthermore, as seen above, while the donation from the alkyne to the $L–Au^I$ moiety is remarkably stable, almost independent of the charge or the nature of the ancillary ligand (phosphane or carbene), the back-donation is quite sensitive to the nature of the auxiliary ligand. Our analysis shows without ambiguity that the metal fragment $L–Au^I$, where L is phosphane, has the greatest overall electron-withdrawing capability because the ligand induces the smallest metal-to-substrate back-donation. In contrast, when L = Cl^- the metal fragment $L–Au^I$ presents the largest back-donation, causing the largest distortion of the coordinated alkyne. These findings explain the X-ray crystallographic structures of the alkynes, which reveal a larger distortion in the case of the neutral complex, one that is progressively reduced on going from carbene to phosphane ligands. These findings thus correlate well with the view that the geometric distortion of a ligand is more strictly related to the back-donation component of the bond.

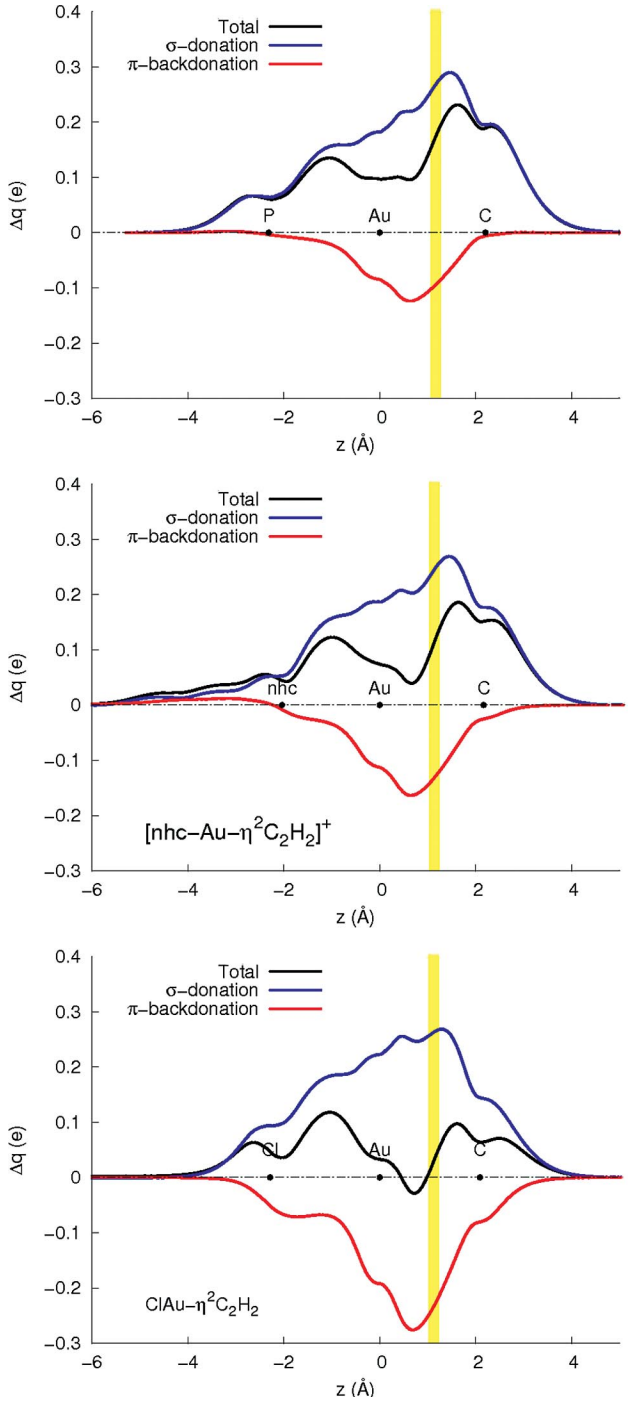

Figure 10. CD curves for the complexes [Cl–Au–ethyne] (**8**), $[NHC–Au–ethyne]^+$ (**11**), and $[PH_3–Au–ethyne]^+$ (**14**). The black dots represent the *z* coordinate of the atoms. The yellow vertical band identifies a suitable boundary between the L–Au and ethyne fragments. Reproduced with permission from ref.[26] Copyright Wiley-VCH Verlag GmbH & Co. KGaA.

Because gold(I) complexes are generally superior π-activating catalysts when compared with analogous complexes of Cu^I and Ag^I, it is clearly of interest to compare the results of the CD analysis of homologous complexes of Au^I, Cu^I, and Ag^I. In general, such comparative studies have indeed been used to try to cast light on the peculiar catalytic properties of gold complexes.[41a,45b] It is typically found, for example, that alkynes coordinated to gold and copper complexes present the largest structural distortions, while silver coordination induces a much smaller effect on the spectroscopic parameters of the alkyne. This type of evidence is confirmed in the simple systems studied by us. For example, we find that ethyne coordinated to gold or copper has the largest distortion/activation (bending from linearity of 17° and 16° and a redshift in the harmonic frequency of the C–C stretching with respect to free ethyne of up to 176 cm^{-1} and 166 cm^{-1}, respectively, for AuCl and CuCl), while in the silver case activation is significantly less pronounced (11° and 107 cm^{-1} in the case of AgCl). The comparative results obtained by the CD analysis are collected and summarized in Table 2, and for the chloride complexes (**9**, **10**) we also report the CD curves in Figure 11. Looking first at the total CD curves, the picture for the lighter coinage metals is very similar to that for the gold complexes, with the curves almost coinciding around the alkyne site. In fact, the net charge on the ethyne, measured at the isodensity boundary, is almost identical for the three coinage metal complexes. This is remarkable and surprising, as it indicates that the net electron-withdrawing power of the three metal fragments towards the unsaturated substrate is essentially the same. Again, if such net Lewis acidity were the sole, or even the major, feature responsible for alkyne activation, we would be at a loss to explain both the differences in catalytic performance and the differences in the structural parameters. But even a cursory inspection of the CD curves for the DCD components immediately clarifies this apparent contradiction, as evident differences emerge among the three metal complexes: the donation component is systematically smaller in the copper and silver complexes than in the gold system, while the metal-to-alkyne back-donation is almost identical (only slightly shifted) in the gold and copper complexes but about half as large in the silver one. This is a fairly general finding, and a similar pattern was observed in the case of the charged complexes NHC–M–alkyne (see Table 2, complexes **11**, **12**, and **13**).

Our analysis thus proves that gold is certainly a superior σ acceptor to the other coinage metals, and this superiority may indeed play a role in explaining its peculiar catalytic performance. But gold is also a strongly back-donating metal, similar if not superior to copper. Therefore the properties and structural changes of the coordinated alkyne are sensitive to the choice of ancillary ligand, as this tunes the back-donation ability of the gold. Gold–phosphane fragments are more acidic than gold–NHC and especially AuCl, because of less back-donation to the substrate (compare complexes **8**, **11**, **14**). These findings are perfectly consistent with the structural information available, which indicates that alkyne distortion due to coordination to cationic metal

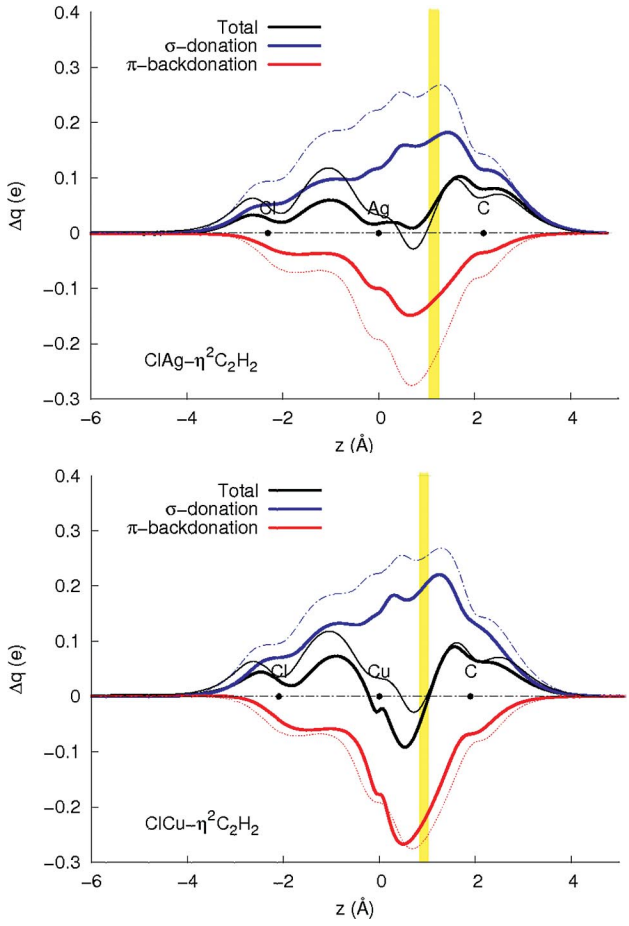

Figure 11. CD curves for the complexes [Cl–M–ethyne] (M = Cu, Ag). The curves for M = Au are also shown for comparison as lighter lines.[26]

fragments such as phosphane–Au^+ or NHC–Au^+ is much less than for neutral metal fragments, because of the reduced back-donating ability of the charged complexes.

We may finally mention that catalytic data show that, in contrast to Ag, Cu does effectively activate some alkyne reactions, revealing a greater similarity to gold than silver. In view of the very similar back-donation pattern between gold and copper, this suggests that the back-donating ability of the metal fragment may in fact play a crucial role in the catalytic cycle.

Conclusions

Although it is now well established that the selectivity of homogeneous Au^I catalysts is influenced by both the ligand and the counterion, a satisfactory explanation of how these factors affect the catalytic cycle is only just beginning to take shape. In this contribution we have reviewed our recent achievements in the characterization of linear gold(I) catalysts binding simple unsaturated systems, of formula [L–Au–S]$^+BF_4^-$, which represent the first intermediate in many gold(I)-catalyzed reactions. Our efforts have concentrated,

in particular, on the study of how the choice of the ligand may affect both the ion-pair structure in solution and the chemical bond between the LAu^I fragment and the substrate, in the attempt to establish a common advanced framework. We have combined state-of-the-art experimental and theoretical tools in order to understand these two important aspects. Two among the most important classes of ligands, differing for their electron-donating ability, have been considered: phosphanes and N-heterocyclic carbenes. State-of-the-art NOE NMR spectroscopic techniques combined with relativistic DFT calculations have been successfully applied for gaining detailed qualitative and quantitative information on the ion pair structure in solution, and we have related this information to the Coulomb potential generated by the $L–Au^I$ fragment. This charge-displacement (CD) analysis of the bond between metal fragment and substrate is a powerful tool that provides a clear and quantitative picture, not only in terms of the net electron-withdrawing property of the metal fragment but, very insightfully, in terms of the donation and back-donation components of the Dewar–Chatt–Duncanson (DCD) model. A poorly donating ligand, such as a phosphane, induces a remarkable acidity in the metal fragment that translates into enhanced electron-withdrawing power towards a coordinated unsaturated substrate. In this case, our results show that the ion-pair structure tends to be well-characterized, with the counterion BF_4^- approaching the cation mainly on the alkyne side. Our recent research has shown that the electronic properties of various P-ligands finely tune the charge accumulation on the alkyne and, consequently, its ability to attract the anion.[59] A NHC ligand, because of its stronger donating ability, induces a much less specific ion-pair structure. This is because the metal fragment, $NHC–Au^+$, has a less acidic character and, consequently, it induces a less pronounced electron depletion at the alkyne site. In the cases studied, the anion displays a propensity to station itself near the imidazole ring of the ligand, far away from the substrate. Within this general pattern, we showed that the ion pairing can be finely tuned with the introduction of functional groups in the ligand. In the case of the phosphane (PPh_3) the introduction of CF_3 groups at the *meta* position of the aromatic ring causes a shift of the counterion from a position near the substrate (position C in Figure 1) to a position near the gold (position B in Figure 1), owing to the acquired acidity of the phenyl *ortho* protons (easily observed in the Coulomb potential). In the case of the NHC compounds, the relative abundance of pairs with the counterion positioned near the imidazole ring (position A) decreases from 83% to 65% when the hydrogen of the imidazole ring is substituted with the less acid methyl fragment. Evidence of counterion effects in the Au^I-catalyzed activation of unsaturated substrates is more pronounced when phosphanes[11,14,16] are used as ancillary ligands instead of NHCs.[12] The more specific ion-pair structure we observed in the phosphane case is fully consistent with this finding, as it should indeed be expected to interfere more easily with the nucleophile attacking the coordinated substrate. Of course, a detailed understanding of the effective role of the counterion can only be achieved after further specific studies that combine structural information about ion pairing in solution, of the kind we presented here, with detailed kinetic data.

The nature of the ancillary ligand not only affects the ion-pairing arrangements, but also directly influences the properties of the chemical bond between gold and an unsaturated substrate. This interplay is very accurately and sensitively evidenced by our theoretical CD analysis, which permits a rigorous definition and assessment of the two bond components at the heart of the popular DCD model: substrate-to-metal donation and metal-to-substrate back-donation. Its application to the gold(I) catalytic intermediates has permitted us to answer conclusively some long-standing questions concerning the nature of the Au^I–carbon bond in these systems. A first important conclusion is that back-donation is a large and important component of the Au^I–substrate bond in all systems, even larger in absolute terms than for the other coinage metals, silver and copper, especially Ag^I. The view that attributes the remarkable catalytic properties of Au^I in activating multiple C–C bonds to a small, or even negligible, back-donation must be abandoned. The back-donation is seen to penetrate the external side of the coordinated substrate, where the nucleophilic attack is directed, thus partially mitigating the electron depletion caused by substrate-to-metal donation. Thus, for example, in the neutral [Cl–Au–ethyne] complex, π back-donation is essentially as large as σ donation. Gold is shown to be a 30–50% better π acceptor (Lewis acid) when coordinating an alkyne than the other coinage metals. While the size of the donation component is surprisingly stable, being largely independent of the ligand, even of its charge, the back-donation is a sensitive and tunable bond component. Furthermore, the computed back-donation proves to be the bond component that has a strong correlation with the geometric distortion of the coordinated alkyne. For example, when the ligand is an anion such as Cl^-, the substrate has a larger geometric distortion than in the case of a cationic metal fragment (with a phosphane or NHC as ligand). Indeed, in the former case, back-donation is much larger, in fact even larger than the donation component. A rational modulation of back-donation through an appropriate choice of ancillary ligand may be used to control the stabilization of specific intermediates (carbocations vs. carbenes) in gold-catalyzed reactions and may be crucial in favoring particular reaction paths. So far we have concentrated our attention on the first intermediate of the catalytic cycle for a limited set of prototype ligands and substrates, but it is clear that the same combined experimental NMR spectroscopic and theoretical approaches could usefully be applied to cast light on the properties of other organogold compounds and intermediates, of the type of intermediate 2 of Scheme 1.[60] A detailed knowledge of ligand effects on the ion-pair structure in solution and on the nature of the gold–carbon chemical bond is a key ingredient for the full understanding of the catalytic cycle and for the design of new, effective catalysts and reaction pathways. The other crucial direction of research must be a more direct probe of the

structure–activity relationships by combining analytical structural information of the kind described here with actual specific kinetic studies, again both experimental and theoretical. Work in this direction is under way in our laboratories.

Supporting Information (see footnote on the first page of this article): Computational details.

Acknowledgments

This work was supported by grants from the Ministero dell'Istruzione, dell'Università e della Ricerca (MIUR, Rome, Italy) and the "Futuro in ricerca" (FIRB) project RBFR1022UQ: Novel Au^{I}-based molecular catalysts: from know-how to know-why (AuCat). Financial support from the Fondazione Cassa di Risparmio di Perugia is also gratefully acknowledged.

[1] a) Z. Li, C. Brouwer, C. He, *Chem. Rev.* **2008**, *108*, 3239 and references therein; b) E. Jiménez-Nùnez, A. M. Echavarren, *Chem. Rev.* **2008**, *108*, 3326 and references therein; c) D. J. Gorin, B. D. Sherry, F. D. Toste, *Chem. Rev.* **2008**, *108*, 3351; d) N. Marion, S. P. Nolan, *Chem. Soc. Rev.* **2008**, *37*, 1776.
[2] A. S. K. Hashmi, *Chem. Rev.* **2007**, *107*, 3180.
[3] W. Wang, G. B. Hammond, B. Xu, *J. Am. Chem. Soc.* **2012**, *134*, 5697.
[4] H. Teller, M. Corbet, L. Mantilli, G. Gopakumar, R. Goddard, W. Thiel, A. Fürstner, *J. Am. Chem. Soc.* **2012**, *134*, 5331.
[5] a) A. Arcadi, *Chem. Rev.* **2008**, *108*, 3266; b) N. Bongers, N. Krause, *Angew. Chem.* **2008**, *120*, 2208; *Angew. Chem. Int. Ed.* **2008**, *47*, 2178.
[6] a) A. S. K. Hashmi, A. M. Schuster, F. Rominger, *Angew. Chem.* **2009**, *121*, 8396; *Angew. Chem. Int. Ed.* **2009**, *48*, 8247; b) Y. Shi, S. D. Ramgren, S. A. Blum, *Organometallics* **2009**, *28*, 1275; c) F. Mohr, L. R. Falvello, M. Laguna, *Eur. J. Inorg. Chem.* **2006**, 833, and references therein; d) D. Weber, M. A. Tarselli, M. R. Gagné, *Angew. Chem.* **2009**, *121*, 5843; *Angew. Chem. Int. Ed.* **2009**, *48*, 5733.
[7] A. Fürstner, M. Alcarazo, R. Goddard, C. W. Lehmann, *Angew. Chem.* **2008**, *120*, 3254; *Angew. Chem. Int. Ed.* **2008**, *47*, 3210.
[8] a) P. Mauleon, R. M. Zeldin, A. Z. Gonzalez, F. D. Toste, *J. Am. Chem. Soc.* **2009**, *131*, 6348; b) I. Alonso, B. Trillo, F. Lopez, S. Montserrat, G. Ujaque, L. Castedo, A. Lledos, J. L. Mascarenas, *J. Am. Chem. Soc.* **2009**, *131*, 13020; H. Teller, S. Flügge, R. Goddard, A. Fürstner, *Angew. Chem.* **2010**, *122*, 1993; *Angew. Chem. Int. Ed.* **2010**, *49*, 1949.
[9] a) H. G. Raubenheimer, H. Schmidbaur, *S. Afr. J. Sci.* **2011**, *107*, art. 459; b) H. G. Raubenheimer, H. Schmidbaur, *Organometallics* **2012**, *31*, 2507.
[10] M. Alcarazo, T. Stork, A. Anoop, W. Thiel, A. Fürstner, *Angew. Chem.* **2010**, *122*, 2596; *Angew. Chem. Int. Ed.* **2010**, *49*, 2542.
[11] a) C. Brouwer, C. He, *Angew. Chem.* **2006**, *118*, 1776; *Angew. Chem. Int. Ed.* **2006**, *45*, 1744; b) M. Schelwies, A. L. Dempwolff, F. Rominger, G. Helmchen, *Angew. Chem.* **2007**, *119*, 5694; *Angew. Chem. Int. Ed.* **2007**, *46*, 5598.
[12] Z. Zhang, R. A. Widenhoefer, *Org. Lett.* **2008**, *10*, 2079.
[13] D. Weber, T. D. Jones, L. Adduci, M. R. Gagné, *Angew. Chem.* **2012**, *124*, 2502; *Angew. Chem. Int. Ed.* **2012**, *51*, 2452.
[14] a) M. A. Tarselli, A. R. Chianese, S. J. Lee, M. R. Gagné, *Angew. Chem.* **2007**, *119*, 6790; *Angew. Chem. Int. Ed.* **2007**, *46*, 6670; b) Y. Xia, A. S. Dudnik, V. Gevorgyan, Y. Li, *J. Am. Chem. Soc.* **2008**, *130*, 6940.
[15] J. Lacour, D. Linder, *Science* **2007**, *317*, 462.
[16] a) G. L. Hamilton, E. J. Kang, M. Mba, F. D. Toste, *Science* **2007**, *317*, 496; b) R. L. LaLonde, B. D. Sherry, E. J. Kang, F. D. Toste, *J. Am. Chem. Soc.* **2007**, *129*, 2452.
[17] M. Bandini, A. Bottoni, M. Chiarucci, G. Cera, G. P. Miscione, *J. Am. Chem. Soc.* **2012**, *134*, 20690.
[18] A. S. K. Hashmi, *Nature* **2007**, *449*, 292.
[19] M. Raducan, M. Moreno, C. Bour, A. M. Echevarren, *Chem. Commun.* **2012**, *48*, 52.
[20] a) D. Kovács, A. Lledós, G. Ujaque, *Organometallics* **2010**, *29*, 5919; b) M. Katari, M. N. Rao, G. Rajaramam, P. Ghosh, *Inorg. Chem.* **2012**, *51*, 5593; c) C. M. Krauter, A. S. Hashmi, M. Pernpointner, *ChemCatChem* **2010**, *2*, 1226.
[21] D. Zuccaccia, S. Sabatini, G. Bellachioma, G. Cardaci, E. Clot, M. Macchioni, *Inorg. Chem.* **2003**, *42*, 5465.
[22] a) D. Zuccaccia, E. Foresti, S. Pettirossi, P. Sabatino, C. Zuccaccia, A. Macchioni, *Organometallics* **2007**, *26*, 6099; b) D. Zuccaccia, A. Macchioni, *Organometallics* **2005**, *24*, 3476.
[23] a) A. Macchioni, A. Romani, C. Zuccaccia, G. Guglielmetti, C. Querci, *Organometallics* **2003**, *22*, 1526; b) D. Zuccaccia, G. Bellachioma, G. Cardaci, C. Zuccaccia, A. Macchioni, *Dalton Trans.* **2006**, 1963.
[24] L. Rocchigiani, C. Zuccaccia, D. Zuccaccia, A. Macchioni, *Chem. Eur. J.* **2008**, *14*, 6589.
[25] L. Belpassi, I. Infante, F. Tarantelli, L. Visscher, *J. Am. Chem. Soc.* **2008**, *130*, 1048.
[26] N. Salvi, L. Belpassi, F. Tarantelli, *Chem. Eur. J.* **2010**, *16*, 7231.
[27] A. Macchioni, *Eur. J. Inorg. Chem.* **2003**, 195 and references therein.
[28] a) D. Zuccaccia, G. Bellachioma, G. Cardaci, G. Ciancaleoni, C. Zuccaccia, E. Clot, A. Macchioni, *Organometallics* **2007**, *26*, 3930; b) A. Macchioni, G. Bellachioma, G. Cardaci, G. Cruciani, E. Foresti, P. Sabatino, C. Zuccaccia, *Organometallics* **1998**, *17*, 5549.
[29] G. Bellachioma, G. Ciancaleoni, C. Zuccaccia, D. Zuccaccia, A. Macchioni, *Coord. Chem. Rev.* **2008**, *252*, 2224.
[30] For reviews on the application of PGSE NMR spectroscopy to the investigation of intermolecular interactions: a) B. Binotti, A. Macchioni, C. Zuccaccia, D. Zuccaccia, *Comments Inorg. Chem.* **2002**, *23*, 417; b) P. S. Pregosin, E. Martinez-Viviente, P. G. A. Kumar, *Dalton Trans.* **2003**, 4007; c) A. Bagno, F. Rastrelli, G. Saielli, *Prog. Nucl. Magn. Reson. Spectrosc.* **2005**, *47*, 41; d) T. Brand, E. J. Cabrita, S. Berger, *Prog. Nucl. Magn. Reson. Spectrosc.* **2005**, *46*, 159; e) Y. Cohen, L. Avram, L. Frish, *Angew. Chem.* **2005**, *117*, 524; *Angew. Chem. Int. Ed.* **2005**, *44*, 520; f) A. Macchioni, G. Ciancaleoni, D. Zuccaccia, C. Zuccaccia, *Chem. Soc. Rev.* **2008**, *37*, 479; g) G. Ciancaleoni, C. Zuccaccia, D. Zuccaccia, A. Macchioni in *Techniques in Inorganic Chemistry* (Eds.: J. P. Fackler Jr., L. R. Falvello), CRC Press, Boca Raton, Fla. USA, **2011**, pp. 129–180; h) G. Ciancaleoni, C. Zuccaccia, D. Zuccaccia, A. Macchioni in *Supramolecular Chemistry: From Molecules to Nanomaterials* (Eds.: P. A. Gale, J. W. Steed), John Wiley & Sons, New York, **2012**, pp. 319–330.
[31] A. Macchioni, *Chem. Rev.* **2005**, *105*, 2039 and references therein.
[32] D. Zuccaccia, L. Belpassi, F. Tarantelli, A. Macchioni, *J. Am. Chem. Soc.* **2009**, *131*, 3170.
[33] D. Zuccaccia, L. Belpassi, L. Rocchigiani, F. Tarantelli, A. Macchioni, *Inorg. Chem.* **2010**, *49*, 3080.
[34] N. Salvi, L. Belpassi, D. Zuccaccia, F. Tarantelli, A. Macchioni, *J. Organomet. Chem.* **2010**, *695*, 2679.
[35] a) C. Zuccaccia, N. G. Stahl, A. Macchioni, M. C. Chen, J. A. Roberts, T. J. Marks, *J. Am. Chem. Soc.* **2004**, *126*, 1448; b) G. Ciancaleoni, N. Fraldi, P. H. M. Budzelaar, V. Busico, A. Macchioni, *Dalton Trans.* **2009**, 8824; c) L. Rocchigiani, G. Bellachioma, G. Ciancaleoni, A. Macchioni, D. Zuccaccia, C. Zuccaccia, *Organometallics* **2011**, *30*, 100; d) L. Rocchigiani, G. Ciancaleoni, C. Zuccaccia, A. Macchioni, *Angew. Chem.* **2011**, *123*, 11956; *Angew. Chem. Int. Ed.* **2011**, *50*, 11752; e)

G. Ciancaleoni, N. Fraldi, P. H. M. Budzelaar, V. Busico, A. Macchioni, *Organometallics* **2011**, *30*, 3096.
[36] B. Binotti, G. Bellachioma, G. Cardaci, C. Carfagna, C. Zuccaccia, A. Macchioni, *Chem. Eur. J.* **2007**, *13*, 1570 and references therein.
[37] S. Macura, R. R. Ernst, *Mol. Phys.* **1980**, *41*, 95.
[38] A. Macchioni, A. Magistrato, I. Orabona, F. Ruffo, U. Rothlisberger, C. Zuccaccia, *New J. Chem.* **2003**, *27*, 455.
[39] E. Clot, *Eur. J. Inorg. Chem.* **2009**, 2319.
[40] a) A. S. K. Hashmi, *Angew. Chem.* **2010**, *122*, 5360; *Angew. Chem. Int. Ed.* **2010**, *49*, 5232; b) H. Schmidbaur, A. Schier, *Organometallics* **2010**, *29*, 2.
[41] a) N. D. Shapiro, F. D. Toste, *Proc. Natl. Acad. Sci. USA* **2008**, *105*, 2779; b) T. J. Brown, M. G. Dickens, R. A. Widenhoefer, *Chem. Commun.* **2009**, 6451; c) T. N. Hooper, M. Green, J. E. McGrady, J. R. Patela, C. A. Russell, *Chem. Commun.* **2009**, 3877; d) T. N. Hooper, M. Green, C. A. Russell, *Chem. Commun.* **2010**, *46*, 2313.
[42] a) T. J. Brown, M. G. Dickens, R. A. Widenhoefer, *J. Am. Chem. Soc.* **2009**, *131*, 6350; b) J. A. Akana, K. X. Bhattacharyya, P. Mueller, J. P. Sadighi, *J. Am. Chem. Soc.* **2007**, *129*, 7736; c) S. Flagge, A. Anoop, R. Goddard, W. Thiel, A. Fürstner, *Chem. Eur. J.* **2009**, *15*, 8558; d) P. de Frémont, N. Marion, S. P. Nolan, *J. Organomet. Chem.* **2009**, *694*, 551.
[43] a) V. Lavallo, G. D. Frey, S. Kousar, B. Donnadieu, G. Bertrand, *Proc. Natl. Acad. Sci. USA* **2007**, *104*, 13569; b) V. Lavallo, G. D. Frey, B. Donnadieu, M. Soleilhavoup, G. Bertrand, *Angew. Chem.* **2008**, *120*, 5302; *Angew. Chem. Int. Ed.* **2008**, *47*, 5224.
[44] a) M. A. Cinellu, G. Minghetti, F. Cocco, S. Stoccoro, A. Zucca, M. Manassero, M. Arca, *Dalton Trans.* **2006**, 5703; b) D. Belli Dell'Amico, F. Calderazzo, R. Dantona, J. Straehle, H. Weiss, *Organometallics* **1987**, *6*, 1207; c) J. A. Flores, R. H. V. Dias, *Inorg. Chem.* **2008**, *47*, 4448; d) R. E. M. Brooner, R. A. Widenhoefer, *Organometallics* **2012**, *31*, 768.
[45] a) J. Wu, P. Kroll, R. H. V. Dias, *Inorg. Chem.* **2009**, *48*, 423; b) R. H. V. Dias, J. A. Flores, J. A. J. Wu, P. Kroll, *J. Am. Chem. Soc.* **2009**, *131*, 11249; c) P. Schulte, U. Behrens, *Chem. Commun.* **1998**, 1633; d) T. J. Brown, R. A. Widenhoefer, *J. Organomet. Chem.* **2011**, *696*, 1216.
[46] a) E. Herrero-Gómez, C. Nieto-Oberhuber, S. López, J. Benet-Buchholz, A. M. Echavarren, *Angew. Chem.* **2006**, *118*, 5581; *Angew. Chem. Int. Ed.* **2006**, *45*, 5455; b) P. Pérez-Galán, N. Delpont, E. Herrero-Gómez, F. Maseras, A. M. Echavarren, *Chem. Eur. J.* **2010**, *16*, 5324.
[47] a) R. A. Sanguramath, T. N. Hooper, C. P. Butts, M. Green, J. E. Grady, C. A. Russell, *Angew. Chem.* **2011**, *123*, 7734; *Angew. Chem. Int. Ed.* **2011**, *50*, 7592; b) R. E. M. Brooner, R. A. Widenhoefer, *Organometallics* **2011**, *30*, 3182.
[48] T. J. Brown, A. Sugie, M. G. Dickens, R. A. Widenhoefer, *Organometallics* **2010**, *29*, 4207.
[49] In addition, it was assumed that the 4 and 1 protons have local correlation times faster than the overall molecular tumbling (τ_c) ($\langle r^{-3}\rangle$) while 8 has a local correlation time slower than τ_c ($\langle r^{-6}\rangle$)

$$\langle r^{-3}\rangle = \left(\frac{1}{N}\sum_{\mu=1}^{N} r_{IS,\mu}^{-3}\right)^{-\frac{1}{3}}$$

$$\langle r^{-6}\rangle = \left(\frac{1}{N}\sum_{\mu=1}^{N} r_{IS,\mu}^{-6}\right)^{-\frac{1}{6}}$$

where μ indicates the different conformations assumed by the spin system. See: J. Tropp, *J. Chem. Phys.* **1980**, *72*, 6035; P. F. Yip, D. A. Case, J. C. Hoch, F. M. Poulsen, C. Redfield, *Computational Aspects of the Study of Biological Macromolecules by Nuclear Magnetic Resonance Spectroscopy*, Plenum Press, New York , **1991**, pp. 317–330.
[50] a) L. N. Appelhans, D. Zuccaccia, A. Kovacevic, A. R. Chianese, J. R. Miecznikowski, A. Macchioni, E. Clot, O. Eisenstein, R. H. Crabtree, *J. Am. Chem. Soc.* **2005**, *127*, 16299; b) L. Busetto, M. C. Cassani, C. Femoni, A. Macchioni, R. Mazzoni, D. Zuccaccia, *J. Organomet. Chem.* **2008**, *693*, 2579.
[51] C. Zuccaccia, A. Macchioni, I. Orabona, F. Ruffo, *Organometallics* **1999**, *18*, 4367.
[52] a) P. Pyykkö, *Angew. Chem.* **2004**, *116*, 4512; *Angew. Chem. Int. Ed.* **2004**, *43*, 4412; b) P. Pyykkö, *Chem. Soc. Rev.* **2008**, *37*, 1967; c) P. Schwerdtfeger, M. Lein, in *Gold Chemistry: Applications and Future Directions in the Life Sciences* (Ed.: F. Mohr), Wiley, New York, **2009**.
[53] D. Benitez, N. D. Shapiro, E. Tkatchouk, Y. Wang, W. A. Goddard, F. D. Toste, *Nat. Chem.* **2009**, *1*, 482.
[54] a) D. Cappelletti, E. Ronca, L. Belpassi, F. Tarantelli, F. Pirani, *Acc. Chem. Res.* **2012**, *45*, 1571; b) L. Belpassi, F. Tarantelli, F. Pirani, P. Candori, D. Cappelletti, *Phys. Chem. Chem. Phys.* **2009**, *11*, 9970; c) L. Belpassi, M. L. Reca, F. Tarantelli, L. F. Roncaratti, F. Pirani, D. Cappelletti, A. Faure, Y. Scribano, *J. Am. Chem. Soc.* **2010**, *132*, 13046.
[55] E. Mizushima, K. Sato, T. Hayashi, M. Tanaka, *Angew. Chem.* **2002**, *114*, 4745; *Angew. Chem. Int. Ed.* **2002**, *41*, 4563.
[56] N. Marion, R. S. Ramon, S. P. Nolan, *J. Am. Chem. Soc.* **2009**, *131*, 448.
[57] a) I. Krossing, *Angew. Chem.* **2011**, *123*, 11781; *Angew. Chem. Int. Ed.* **2011**, *50*, 11576; b) D. J. Gorin, F. D. Toste, *Nature* **2007**, *446*, 395.
[58] H. V. R. Dias, C. Dash, M. Yousufuddin, M. A. Celik, G. Frenking, *Inorg. Chem.* **2011**, *50*, 4253; A. J. Lupinetti, S. Fau, G. Frenking, S. H. Strauss, *J. Phys. Chem. A* **1997**, *101*, 9551.
[59] G. Ciancaleoni, L. Belpassi, F. Tarantelli, D. Zuccaccia, A. Macchioni, *Dalton Trans.* **2013**, *42*, 4122.
[60] a) L. Liu, G. B. Hammond, *Chem. Soc. Rev.* **2012**, *41*, 3129; b) R. Döpp, C. Lothchütz, T. Wurm, M. Pernpointner, S. Keller, F. Rominger, A. S. Hashmi, *Organometallics* **2011**, *30*, 5894.

Received: February 28, 2013
Published Online: June 13, 2013

